N-Terminal Deletions Modify the Cu^{2+} Binding Site in Amyloid-β†

Jesse W. Karr,‡ Henrietta Akintoye,‡ Lauren J. Kaupp,§ and Veronika A. Szalai*,‡

Department of Chemistry & Biochemistry, University of Maryland, Baltimore County, 1000 Hilltop Circle, Baltimore, Maryland 21250, and Department of Oceanography, University of Hawai'i at Manoa, 1000 Pope Road, Marine Sciences Building, Honolulu, Hawaii 96822

Received November 11, 2004; Revised Manuscript Received February 9, 2005

ABSTRACT: Copper is implicated in the in vitro formation and toxicity of Alzheimer's disease amyloid plaques containing the β-amyloid (Aβ) peptide (Bush, A. I., et al. (2003) *Proc. Natl. Acad. Sci. U.S.A. 100,* 11934). By low temperature electron paramagnetic resonance (EPR) spectroscopy, the importance of the N-terminus in creating the Cu^{2+} binding site in native Aβ has been examined. Peptides that contain the proposed binding site for Cu^{2+}—three histidines (H6, H13, and H14) and a tyrosine (Y10)—but lack one to three N-terminal amino acids, do not bind Cu^{2+} in the same coordination environment as the native peptide. EPR spectra of soluble Aβ with stoichiometric amounts of Cu^{2+} show type 2 Cu^{2+} EPR spectra for all peptides. The ligand donor atoms to Cu^{2+} are 3N1O when Cu^{2+} is bound to any of the Aβ peptides (Aβ16, Aβ28, Aβ40, and Aβ42) that contain the first 16 amino acids of full-length Aβ. When a Y10F mutant of Aβ is used, the coordination environment for Cu^{2+} remains 3N1O and Cu^{2+} EPR spectra of this mutant are identical to the wild-type spectra. Isotopic labeling experiments show that water is not the O-atom donor to Cu^{2+} in Aβ fibrils or in the Y10F mutant. Further, we find that Cu^{2+} cannot be removed from Cu^{2+}-containing fibrils by washing with buffer, but that Cu^{2+} binds to fibrils initially assembled *without* Cu^{2+} in the same coordination environment as in fibrils assembled *with* Cu^{2+}. Together, these results indicate (1) that the O-atom donor ligand to Cu^{2+} in Aβ is not tyrosine, (2) that the native Cu^{2+} binding site in Aβ is sensitive to small changes at the N-terminus, and (3) that Cu^{2+} binds to Aβ fibrils in a manner that permits exchange of Cu^{2+} into and out of the fibrillar architecture.

The role of metal ions in plaque formation and neurodegeneration in Alzheimer's disease (AD[1]) might be an important factor in the pathophysiology of the disease (*1*−*4*). Fibrils, a constituent of AD plaques, are composed of the 39−42 amino acid β-amyloid peptide (Aβ) and are thought to be linked to neurodegeneration in AD (*5*−*7*). Metal ions are found in plaques from AD patients' brains (*8*, *9*) and have been shown to bind to Aβ in vitro (*1*, *10*−*15*). There are three principal proposals for the involvement of transition metal ions in AD neuropathology, all of which may be operative in AD to some degree. The first proposal is that transition metal ions affect the aggregation rate (*3*, *15*−*18*) or type of Aβ aggregate formed (*19*). The second proposal is that redox-active metals induce neurotoxicity by direct chemical reaction with Aβ (*11*, *20*−*23*). Specifically, a methionine residue (M35) in Aβ40 reportedly reduces Cu^{2+} to Cu^{1+}, which traps O_2 to produce H_2O_2 (*21*, *23*). The third proposal is that metal ions modify fibril morphology, inducing distinct plaque structures. This effect has been observed for Zn^{2+} (*15*) and is consistent with the proposal that plaque structure rather than plaque amount determines disease severity (*24*). Based on the assumption that metal ions contribute to AD, a new AD therapy involves administration of a metal ion chelator to decrease the metal ion-dependent reactivity of Aβ and to release Aβ from plaques (*25*, *26*). This metal ion chelator decreases deposition of Aβ in the brains of transgenic mice (*27*) and releases soluble Aβ from preformed amyloid deposits (*28*), supporting the finding that metal ions are found in AD plaques in vivo. A detailed knowledge of the coordination geometries and binding sites of relevant metal ions as well as the mechanism through which metal ions participate in fibrillization events will aid selective chelation therapy as a means to combat AD (*25*).

The coordination environment of Cu^{2+} in Aβ for both soluble peptide and aggregates, including senile plaques, has been shown to be nitrogen rich by electron paramagnetic resonance (EPR) and Raman spectroscopies (*9*, *11*−*13*, *20*, *22*, *29*−*32*). For the peptides Aβ40 or Aβ28 with Cu^{2+}, EPR spectroscopy indicates that the ligand donor atom set to Cu^{2+} is 3N1O (*11*, *20*, *33*). Based on this ligand donor atom set, three histidines (H6, H13, H14) and tyrosine (Y10) have been proposed as ligands to Cu^{2+} in Aβ (*11*, *20*). Raman measurements on Cu^{2+}-containing Aβ aggregates show that histidine is coordinated to Cu^{2+} (*9*, *12*), suggesting that Cu^{2+} might cross-link peptide strands in aggregates via coordination to histidines, a binding mode that has been proposed

† Supported by an Alzheimer's Disease Research Pilot Project Award from the American Health Assistance Foundation (A2003-227) and the Designated Research Initiative Fund of UMBC.

* Author to whom correspondence should be addressed. Phone: 410-455-1576. Fax: 410-455-2608. E-mail: vszalai@umbc.edu.

‡ University of Maryland.

§ University of Hawai'i at Manoa.

[1] Abbreviations: AD, Alzheimer's disease; Aβ, β-amyloid peptide; BC, bathocuproine disulfonic acid; EDTA, ethylenediamine tetraacetic acid; EGTA, ethyleneglycol tetraacetic acid; TEM, transmission electron microscopy; EPR, electron paramagnetic resonance; HFIP, 1,1,1,3,3,3-hexafluoro-2-propanol; ThT, thioflavin T; TPEN, *N*,*N*,*N*′,*N*′-tetrakis-(2-pyridylmethyl)ethylenediamine.

10.1021/bi047611e CCC: $30.25
Published on Web 03/17/2005

Table 1: Sequences of Aβ Peptides

peptide	sequence
Aβ42	DAEFRHDSGYEVHHQKLVFFAEDVGSN-KGAIIGLMVGGVVIA
Aβ40	DAEFRHDSGYEVHHQKLVFFAEDVGSN-KGAIIGLMVGGVV
Aβ28	DAEFRHDSGYEVHHQKLVFFAEDVGSNK
Aβ16	DAEFRHDSGYEVHHQK
Aβ16Y10**F**	DAEFRHDSG**F**EVHHQK
Aβ2-16	AEFRHDSGYEVHHQK
Aβ4-16	FRHDSGYEVHHQK
Aβ4-16Y10**F**	FRHDSG**F**EVHHQK

for Zn^{2+} in fibrillar Aβ (*15*, *34*). Although Raman spectroscopy of Aβ aggregates formed in vitro in the presence of Cu^{2+} suggests tyrosinate coordination to Cu^{2+} (*12*), Raman microscopy of senile plaques from AD patients does not (*9*). Potentiometric titrations of Aβ16 and Aβ28 with Cu^{2+} show no evidence of tyrosine phenolate coordination, but substantiate H13 and H14 ligation to Cu^{2+} at neutral pH (*32*). Similarly, NMR spectroscopy of Aβ28 shows that tyrosine is not a ligand to Cu^{2+} and that histidines are important in creating the native Cu^{2+} binding site (*33*). Further support for histidine and tyrosine as metal ion ligands is derived from aggregation experiments with modified Aβ peptides and metal ions. The modified peptides are rat Aβ (*35*), which does not contain Y10 or H13, mutated Aβ (*15*, *35*), in which H13 has been replaced by glutamine, or chemically modified Aβ (*11*, *15*), in which the histidines have been methylated. All of these peptides display altered aggregation behavior in the presence of metal ions, suggesting that both Y10 and H13 are important in metal ion-induced aggregation events and that these residues could be ligated directly to metal ions.

To probe the proposed three histidine/one tyrosine coordination environment of Cu^{2+} in Aβ, we have used Aβ peptides of varying length and composition in conjunction with tyrosine fluorescence measurements and low temperature electron paramagnetic resonance (EPR) spectroscopy. We find that tyrosine fluorescence intensity in Aβ is not quenched entirely, as would be expected for direct coordination of the tyrosine phenolic oxygen to Cu^{2+}. All of the peptides display type 2 Cu^{2+} EPR spectra, but the ligand donor atoms to Cu^{2+} vary depending on the sequence of the peptide. A Y10F mutant of Aβ has the same Cu^{2+} ligand donor atom set as the native peptide. This finding substantiates other work showing that the O-atom donor ligand to Cu^{2+} in Aβ is not tyrosine (*32*, *33*) and is important given a recently proposed mechanism for Cu^{2+}-induced neurotoxicity of Aβ predicated on Cu^{2+} ligation by Y10 (*30*). Spectra of samples prepared in $H_2{}^{17}O$ show that water is not a ligand to Cu^{2+} in Aβ40 fibrils or the Y10F mutant. Finally, when Cu^{2+} is added to Aβ40 fibrils that initially do not contain Cu^{2+}, an EPR spectrum like that for Cu^{2+}-containing Aβ40 fibrils is produced. These results support the idea that Cu^{2+} binds near the N-terminus in both soluble and fibrillar Aβ and show that Cu^{2+} can be incorporated into metal-free fibrils, a process that has not been demonstrated previously.

MATERIALS AND METHODS

Materials. Peptides were purchased from Bachem (King of Prussia, PA), Sigma-Genosys (The Woodlands, TX), or rPeptide (Athens, GA). Table 1 lists the sequences of the Aβ peptides. Biological grade glycerol, Tris, HFIP, and sodium chloride were purchased from Fisher. Quartz EPR tubes were purchased from Wilmad (Buena, NJ). Solutions were prepared in MilliQ water (resistivity > 18 mΩ, total organic content < 35 ppb).

Sample Preparation Protocols. Peptide was monomerized with hexafluoroisopropanol (HFIP) according to literature procedures and stored at −80 °C in HFIP (*36*, *37*). The peptide in HFIP was removed with a Hamilton gastight syringe that had been washed with multiple volumes of HFIP. Immediately prior to use of peptide, HFIP was removed using a spin-vacuum system. Preparation of samples by dissolution in HFIP followed by removal of HFIP produces homogeneous solutions of monomeric peptide (*38*).

Samples of soluble Aβ were prepared by dissolving dried peptide in buffer containing 100 mM Tris, 150 mM NaCl, pH 7.4 or 50 mM NaPi, 75 mM NaCl, pH 7.2. The peptides Aβ16, Aβ4-16, and Aβ4-16Y10F do not contain the fibrillization domain consisting of residues 16−21 (*39*−*43*). It has been reported that Aβ16 does not fibrillize in the presence of Cu^{2+} at pH 7.4 (*12*), and no evidence for Aβ4-16 or Aβ4-16Y10F fibrillization at pH 7.4 in the presence of Cu^{2+} was detected by ThT assay (data not shown). Samples for EPR spectroscopy were dissolved in buffer containing 50% glycerol (v/v). Inclusion of glycerol as a cryoprotectant for biological samples is an accepted method for minimizing artifactual dipolar interactions between paramagnets and protecting sample fidelity (*44*, *45*). We have previously shown that inclusion of glycerol does not affect the EPR properties of Cu^{2+} bound to Aβ (*31*). After peptide was resuspended in buffer, but prior to addition of Cu^{2+}, an aliquot of the sample was removed for peptide concentration determination. Peptide concentrations were determined on the basis of the absorbance at 214 nm using a calibration curve generated with BSA standards from Sigma.

The appropriate concentration of a Cu^{2+} stock solution in buffer was added to the remainder of the peptide sample. The sample was vortexed, transferred to a quartz EPR tube (*11*, *20*), and frozen to 77 K prior to data collection. The time between addition of Cu^{2+} to the peptide and freezing of the sample is not sufficient to generate a substantial concentration of β-sheets as detected by ThT fluorescence assay (*46*).

For fibrillar samples, the peptide as prepared above in buffer was incubated at 37 °C for 7−14 days without agitation in the absence or presence of Cu^{2+}. Samples were then assayed for fibril formation by transmission electron microscopy and ThT fluorescence. Fibrils for EPR experiments were separated by centrifugation (30 min, 16000 rcf), washed once with 100 μL of 100 mM Tris, 150 mM NaCl, pH 7.4 with 50% glycerol (v/v) or 50 mM NaPi, 75 mM NaCl, pH 7.2 containing 50% glycerol (v/v), and resuspended in 100 μL of the same buffer.

The $^{63,65}Cu^{2+}$ stock solution was generated by dissolution of cleaned copper wire in nitric acid and water. The Cu^{2+} concentrations in samples were determined by EPR spectroscopy based on a calibration curve generated from Cu^{2+} standards in 100 mM Tris, 150 mM NaCl, pH 7.4 with 50% glycerol (v/v). The concentration of Cu^{2+} in the Cu^{2+} EPR standards was assayed by chelation with bathocuproine disulfonic acid (BC) and reduction with ascorbate (*47*). The

quantity of total copper as $[Cu(BC)_2]^{3-}$ was quantified using $\epsilon_{483} = 12500\ M^{-1}\ cm^{-1}$ (*47*). The 0, 50, and 100 μM Cu^{2+} standards contained 0.0 ± 0.7, 54.0 ± 1.0, and 108.4 ± 0.6 μM Cu^{2+}, respectively.

Samples for experiments with $H_2{}^{16}O$ vs $H_2{}^{17}O$ were prepared by dissolving 1 mg of Aβ40 in 1 mL of HFIP. The solution was split in half, and the two 500 μL samples were dried in a speed-vacuum system. Once dried, 12 μL of 1 M Tris, 1.5 M NaCl in $H_2{}^{16}O$ and 108 μL of water (either $H_2{}^{16}O$ or 35−40% enriched $H_2{}^{17}O$) was added and the samples were vortexed. A 20 μL aliquot of each sample was removed and the peptide concentration determined against a BSA protein concentration calibration curve. After the peptide concentration was determined, 0.9 molar equiv of copper was added to the remaining 100 μL of each sample. For fibrils, a 50 μL aliquot was removed from each sample for ThT assay and the remainder of the sample was used to prepare EPR samples. Both ThT assay and EPR samples were placed in a 37 °C heating block for 14 days without agitation. The calculated peptide concentration was 309.4 μM for the sample prepared in $H_2{}^{16}O$ and 362.5 μM for the fibrils prepared in $H_2{}^{17}O$. Approximately 50 μL of glycerol was added to each EPR sample; the samples were vortexed, transferred to quartz EPR tubes, and frozen to 77 K before data collection.

Thioflavin T Assay. Samples were assayed for β-sheet formation using the procedure outlined by Levine (*46*). Briefly, 5−15 μL of sample was mixed with 3 mL of buffer containing 5 μM ThT in 50 mM glycine−NaOH, pH 8.5 (ThT assay buffer). Each sample was assayed in triplicate. In some cases, samples were centrifuged (30 min, 16100 rcf) and 70−90% of the supernatant removed. The remaining volume (typically 20 μL) was vortexed and 5 μL added to 3 mL of ThT assay buffer. This method was developed to ensure that even low concentrations of β-sheet containing species could be detected. Supernatants from these assays contained β-sheet amounts below the detection limit of the ThT assay (*46*). Spectra were collected on a Jobin-Yvon SPEX Fluoromax II fluorometer using a 1 cm path length cuvette and the following conditions: wavelength range, 600−460 nm; integration time, 0.100 s; excitation slit width of 5 nm; emission slit width of 10 nm. The excitation wavelength was 446 nm, and spectra are an average of three scans.

Tyrosine Fluorescence. Spectra were collected on a Jobin-Yvon SPEX Fluoromax II fluorometer using a 1 or 0.3 cm path length cuvette and the following conditions: integration time, 0.100 s; excitation slit width of 5 nm; emission slit width of 5 nm. The excitation wavelength was 278 nm, and spectra are an average of three scans. Monomeric peptide samples were prepared at a concentration of 10 μM in 100 mM Tris, 150 mM NaCl, pH 7.4. The buffer used for these experiments was stored in acid-washed glass bottles to ensure that fluorescent compounds leached from plasticware did not interfere with the fluorescence measurements. Aliquots of a $^{63,65}Cu^{2+}$ solution in 100 mM Tris, 150 mM NaCl, pH 7.4 buffer were added to the peptide; the total volume change did not exceed 10%. At least three separate trials were performed for each peptide.

Electron Microscopy. Electron microscopy images were collected at the University of Maryland, Baltimore Dental School with a JEOL JEMEX II transmission electron microscope. Samples were placed on 300 mesh Formvar films and stained with 1% phosphotungstic acid.

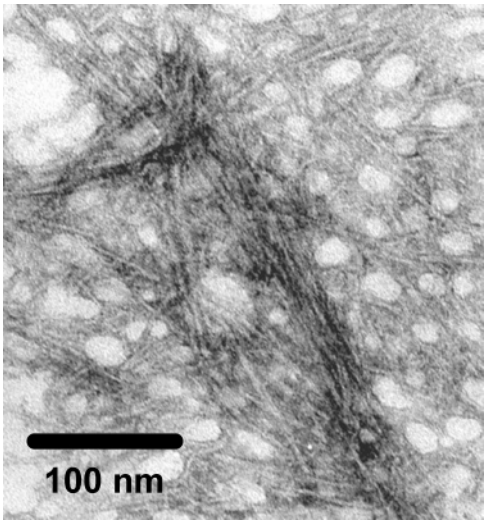

FIGURE 1: TEM image of Aβ40 fibrils formed in the presence of Cu^{2+} in pH 7.2 phosphate buffer. Samples were negatively stained with 1% phosphotungstic acid. Magnification: 60000×.

EPR Spectroscopy. EPR spectra were collected on a Bruker EMX 6/1 spectrometer equipped with a microwave frequency meter and an Oxford Instruments ESR900 liquid He cryostat system. Spectral collection parameters are in the figure captions. Errors given for the peak widths at half-height are based on relative errors for the peak heights based on signal-to-noise measurements.

RESULTS

An electron microscopy image of Aβ40 fibrils assembled in the presence of 0.9 molar equiv of Cu^{2+} in 50 mM NaPi, 75 mM NaCl, pH 7.2 buffer and stained with 1% phosphotungstic acid is shown in Figure 1. The filaments are 5.5 ± 0.9 nm in width, which is similar to those assembled without Cu^{2+} (*48*, *49*) or with Cu^{2+} but in 100 mM Tris, 150 mM NaCl, pH 7.4 buffer (*31*). The literature on pH and Aβ aggregate formation indicates that $5.5 < pH < 6.5$ is optimal for aggregation/fibrillization involving metal ions (*15*, *17*). Because pH 7.4 has been shown to promote Aβ fibril formation over the production of amorphous aggregates in vitro (*36*) and the EPR parameters of Cu^{2+} bound to Aβ in pH 6.9 (*11*) or pH 7.0−8.0 buffers (*20*, *29*) are the same, pH 7.2−7.4 buffers were used here. At pH 7.2 in phosphate buffer or pH 7.4 in Tris buffer, Aβ incubated with Cu^{2+} produces fibrils discernible by electron microscopy (*31*). These fibrils contain one Cu^{2+} ion per peptide based on previous inductively coupled plasma mass spectrometry and amino acid analysis measurements (*31*).

The apparent binding affinities of Cu^{2+} for Aβ40, Aβ28, Aβ16, and Aβ4-16 in our buffers were determined by tyrosine fluorescence, which is quenched in the presence of bound Cu^{2+}, making it a convenient means to follow metal ion binding (*14*, *50*). Representative tyrosine fluorescence intensity data as a function of Cu^{2+} concentration are shown in Figure 2 along with fits and residuals for a single-site binding isotherm. A two-site binding isotherm did not improve the fits. In addition, Job plots (method of continuous variation analysis (*51*)) of Cu^{2+} with Aβ28 show that the peptide:Cu^{2+} stoichiometry is 1:1 (data not shown). Garzon-

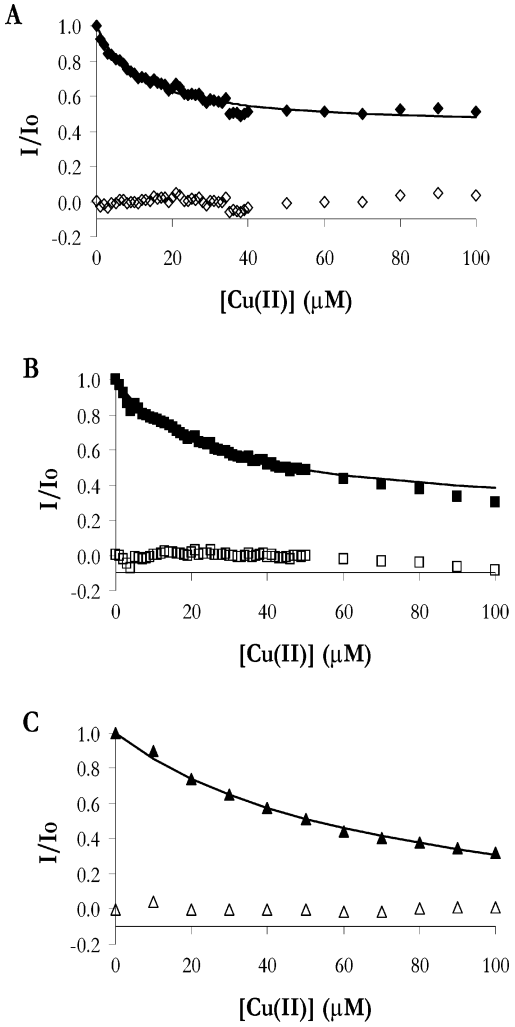

FIGURE 2: Decrease in tyrosine fluorescence as a function of added Cu^{2+} for (A) 10 μM Aβ40, (B) 10 μM Aβ28, and (C) 10 μM Aβ16 in 100 mM Tris, 150 mM NaCl, pH 7.4. Data were fit to a one-site binding isotherm as described in Materials and Methods. Open symbols in each of the panels are the residuals for the fits.

Rodriguez et al. have determined previously that Aβ40 and Aβ42 bind one Cu^{2+} ion per peptide using this method (*14*). Decreasing the Tris buffer concentration from 100 mM to 10 mM gave similar apparent dissociation constants. Tyrosine fluorescence spectra and ThT assays showing that no detectable fibrillization occurs over the duration of the fluorescence experiments (2 h) are given in the Supporting Information (Figures S1 and S2, respectively). The emission maximum of tyrosine in the peptides does not shift upon the addition of Cu^{2+} (Figure S1), which is evidence against the formation of tyrosinate ($\lambda_{em\ max} = 345$ nm (*50*)).

All of the peptides bind Cu^{2+} with apparent dissociation constants in the micromolar range (Table 2). These apparent dissociation constants were determined in the presence of Tris, which depresses the measured affinities of Cu^{2+} for Aβ compared to those determined by potentiometric titrations (*32*) or competition experiments (*10*). Thus, our apparent dissociation constants only indicate *relative* Cu^{2+} affinities for the Aβ peptides under our conditions. The Cu^{2+} affinity under our conditions is highest for Aβ40 and decreases as the peptide length decreases. The exception is Aβ4-16, the shortest peptide, which has an apparent affinity for Cu^{2+} comparable to that of Aβ40. We attribute the difference in apparent affinity between Aβ4-16 and the other Aβ peptides to a change in Cu^{2+} binding environment in Aβ4-16 as determined by EPR spectroscopy (see below).

Table 2: Apparent Cu^{2+} Binding Affinities and EPR Parameters for Aβ Peptides[a]

sample	K_d^{app} (μM)	$A_{\|}$	$g_{\|}$	$g_\perp$
Aβ42	nd[b]	168 ± 2	2.265 ± 0.002	2.062
Aβ40	11 ± 1	170 ± 4	2.265 ± 0.004	2.059
Aβ28	28 ± 5	169 ± 1	2.269 ± 0.001	2.060
Aβ16	47 ± 5	171 ± 1	2.266 ± 0.001	2.059
Aβ16Y10F	na[c]	173 ± 3	2.264 ± 0.003	2.061
Aβ2-16	nd	166 ± 2[d]	2.266 ± 0.002[d]	nd
		153 ± 3	2.226 ± 0.003	nd
Aβ4-16	8 ± 2	206 ± 1	2.178 ± 0.001	2.049
Aβ4-16Y10F	na	204 ± 0	2.180 ± 0.001	2.051

[a] Apparent dissociation constants were determined in 100 mM Tris, 150 mM NaCl, pH 7.4 buffer. EPR parameters were determined in 50 mM NaP_i, 75 mM NaCl, pH 7.2 buffer containing 50% glycerol (v/v). [b] Not determined. [c] Not applicable. [d] Minor component in spectrum.

The tyrosine fluorescence intensity of Aβ peptides is not quenched entirely in the presence of Cu^{2+}. At the end of a titration, the intensity plateaus at about 30−45% of the initial tyrosine intensity (Figure 2). Aβ does not contain tryptophan, and phenylalanine fluorescence is not expected to contribute to the overall fluorescence. The quantum yield for phenylalanine fluorescence is very low and the fluorescence maximum is blue-shifted relative to that for tyrosine (*52*). We confirmed that phenylalanine content does not contribute to Aβ fluorescence by measuring the fluorescence intensities of matched concentrations of Aβ16, which contains one phenylalanine, Aβ28, which contains all three phenylalanines of the native sequence, and Aβ16Y10F, which contains two phenylalanines. If phenylalanine fluorescence contributes to the overall Aβ fluorescence, the initial fluorescence intensities should vary based on phenylalanine content. The initial fluorescence intensities of Aβ16 and Aβ28 differ by no more than 10% and that of Aβ16Y10F is only 5% larger than background fluorescence from buffer (data not shown). Thus, the lack of complete Aβ tyrosine fluorescence quenching observed in the presence of Cu^{2+} is not due to background phenylalanine fluorescence.

To show that peptides are not contaminated with adventitious Cu^{2+} (or other metal ions) prior to titrations, initial tyrosine fluorescence intensities were measured without and with 1 mM EDTA (Supporting Information Figure S3). Within error, the intensities are the same, showing that Cu^{2+} (or other metal ions) is not bound to the peptides in a binding site that affects tyrosine fluorescence prior to the titration.

Low-temperature EPR spectroscopy of Cu^{2+}-containing proteins is an accepted method for determining Cu^{2+} coordination environment (*53*). In the case of Aβ peptides, optical methods for elucidating Cu^{2+} ligand donor atoms are less robust because of the propensity for the full-length peptides to aggregate and cause significant light scattering and decreased spectral resolution. Figure 3 shows 20 K EPR spectra of Aβ peptides bound to Cu^{2+} in phosphate buffer at pH 7.2. Spectra for Aβ40, Aβ28, Aβ16, and Aβ16Y10F are nearly identical (Figure 3A), with slight differences in the $g_\perp$ region of the spectra. These spectra indicate a similar ligand donor atom set for Cu^{2+} in these peptides and support the proposal that the Cu^{2+} binding site is in the first 16 residues of the full-length Aβ40 peptide (*11*, *20*, *29*, *32*).

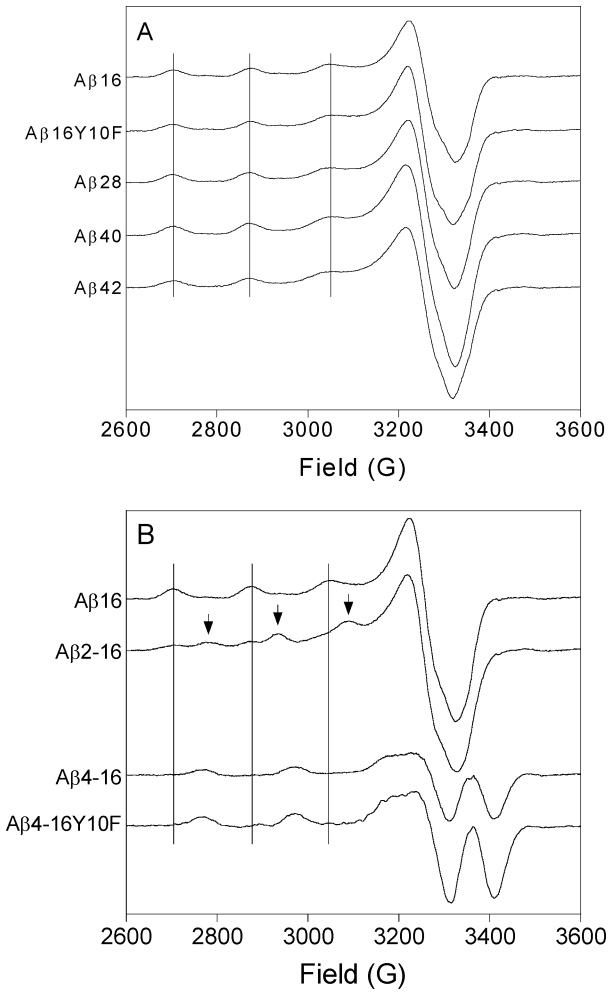

FIGURE 3: (A) 20 K EPR spectra of 100 μM Aβ peptides in the presence of 90 μM Cu^{2+} in 50 mM NaPi, 75 mM NaCl, pH 7.2 buffer containing 50% glycerol (v/v). (B) 20 K EPR spectra of 100 μM Aβ peptides with N-terminal deletions in the presence of 90 μM Cu^{2+} in 50 mM NaPi, 75 mM NaCl, pH 7.2 buffer containing 50% glycerol (v/v). The arrows in the Aβ2-16 spectrum indicate the Cu^{2+} hyperfine peaks assigned to the major component. All spectra were collected with the following experimental parameters: microwave frequency = 9.38 GHz, microwave power = 0.5 mW, modulation amplitude = 10 G, time constant = 40.96 ms, conversion time = 40.96 ms, gain = 5×10^4, eight scans.

The EPR signal for Cu^{2+} bound to soluble Aβ28 at equimolar concentrations in pH 7.2 phosphate buffer exhibits a Curie temperature dependence, as does the EPR signal for Cu^{2+} bound to Aβ40 fibrils assembled in pH 7.2 phosphate buffer (Supporting Information, Figures S4 and S5, respectively). Thus, our previous results for Cu^{2+} bound to Aβ in Tris buffer showing that Cu^{2+} is in a mononuclear metal ion binding site (*31*) are reproduced in phosphate buffer.

The spectra for Aβ peptides with N-terminal deletions (Figure 3B) differ significantly from those for Aβ peptides containing the first 16 amino acids of the native Aβ sequence. These results are surprising because Aβ2-16 and Aβ4-16 contain the three histidines and tyrosine proposed as ligands to Cu^{2+} in native Aβ (*11*, *20*, *29*). The spectrum of Cu^{2+} with Aβ2-16 contains a mixture of species. The minor component aligns well with the spectrum for Cu^{2+} bound to Aβ16. The major component (marked with arrows in Figure 3B) has a much smaller hyperfine peak splitting than that found for Cu^{2+} bound to the peptides in Figure 3A. Aβ4-16 or Aβ4-16Y10F with Cu^{2+} produce spectra that are similar to one another, but these spectra do not resemble those for Cu^{2+} bound to Aβ16, Aβ28, Aβ40, or Aβ42 because the hyperfine peak splitting is much larger.

EPR parameters, $g_{||}$ and $A_{||}$, for the spectra in Figure 3A are in Table 2 and are consistent with 3N1O coordination for the peptides Aβ16, Aβ16Y10F, Aβ28, Aβ40, and Aβ42. The 3N1O coordination environment for Cu^{2+} bound to Aβ corroborates that previously reported (*11*, *20*, *22*, *29*−*31*, *33*) and confirms that Aβ16 can be used to model the Cu^{2+} binding site in full-length Aβ (*12*, *32*). The $A_{||}$ and $g_{||}$ values for Aβ40 and Aβ28 in the presence of Cu^{2+} are very similar to those obtained by Huang et al. (*20*) (Cu^{2+} with Aβ40 pH 7.4: $g_{||} = 2.295$, $A_{||} = 163.60$ cm^{-1})[2] and Curtain et al. (*11*) (Cu^{2+} with Aβ28 pH 6.9: $g_{||} = 2.295$, $A_{||} = 15.9$ millikaisers (170 G)[2]). The parameters for Cu^{2+} bound to Aβ16 almost exactly match those for the dominant Cu^{2+}-Aβ16 species at pH 7 reported by Kowalik-Jankowska et al. (*32*) (Cu^{2+} with Aβ16: $g_{||} = 2.262$, $A_{||} = 175$ G for CuHL). In addition, the EPR parameters reported by Syme et al. ($g_{||} = 2.26$, $A_{||} = 177$ G) for the dominant 3N1O component in spectra of Aβ16 or Aβ28 with Cu^{2+} at $5 < \text{pH} < 8-9$ also are very similar (*33*). It appears that there is now consensus regarding the EPR features of the major Cu^{2+}-Aβ peptide component even though all of the measurements have been made under slightly different solution conditions. The $g_{||}$ and $A_{||}$ values for Aβ4-16, Aβ4-16Y10F, and Aβ2-16 also are in Table 2. The minor component in the spectrum of Cu^{2+} with Aβ2-16 has $A_{||}$ and $g_{||}$ values that indicate 3N1O coordination. The major component $A_{||}$ and $g_{||}$ values are difficult to assign to a coordination environment from Blumberg−Peisach plots (*53*), but these EPR parameters are very similar to those reported for the 3N1O Cu^{2+} complex of Aβ16 at pH 8 ($A_{||} = 156$ G, $g_{||} = 2.229$). In that case, the amino terminus, a histidine, a carbonyl group, and a deprotonated amide have been assigned as ligands to Cu^{2+} (*32*). These parameters also are similar to those observed for Cu^{2+} bound to prion peptides ($g_{||} = 2.23$, $A_{||} = 148-160$ G) where Cu^{2+} is bound to histidine, a backbone carbonyl, and two deprotonated amides (*44*). Thus, it is possible that the major component in the EPR spectrum of Cu^{2+} bound to Aβ2-16 is also 3N1O, but contains a deprotonated amide in its coordination sphere. The $A_{||}$ and $g_{||}$ values for Aβ4-16 and Aβ4-16Y10F, which lack the three N-terminal amino acids (DAE) of Aβ16, establish the coordination environment for Cu^{2+} as 4N (*53*). Almost identical EPR parameters have been observed for native Cu^{2+}−Aβ complexes at high pH in which one histidine and three deprotonated amides (4N) are ligands to Cu^{2+} (*32*).

The location of Cu^{2+} in fibrils, specifically whether Cu^{2+} is bound to the inside or outside, is a major unresolved question, the answer to which has significant impact on proposals of the mechanism through which Cu^{2+} participates in fibrillization. The data in Figures 4−6 address the issue of Cu^{2+} binding location in fibrils. For data in Figure 4, fibrils assembled with a molar excess of Cu^{2+} were separated from the parent solution by centrifugation. The supernatant of this

[2] The units of $A_{||}$ for Cu^{2+} bound to Aβ40 reported by Huang et al. (*20*) are given as cm^{-1}; the correct unit is probably Gauss. The reported value in millikaisers was converted to Gauss using the conversion factor 0.09348 (*45*).

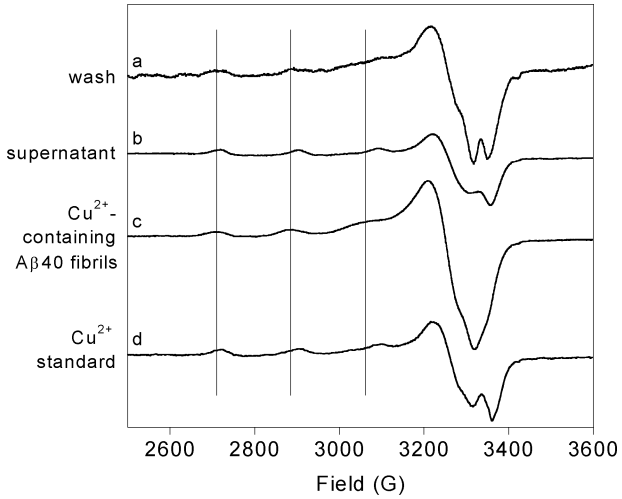

FIGURE 4: 10 K EPR spectra of 25 μM Cu^{2+} standard (spectrum d), Aβ40 fibrils containing Cu^{2+} (spectrum c), fibrillar supernatant retained after the initial centrifugation step to isolate fibrils (spectrum b), and the aliquot of buffer used to wash fibrils after isolation (spectrum a). The buffer for all samples was 100 mM Tris, 150 mM NaCl, pH 7.4 containing 50% glycerol (v/v). EPR parameters: microwave frequency = 9.38 GHz, microwave power = 0.5 mW, modulation amplitude = 10 G, time constant = 40.96 ms, conversion time = 40.96 ms, gain = 5×10^4, eight scans.

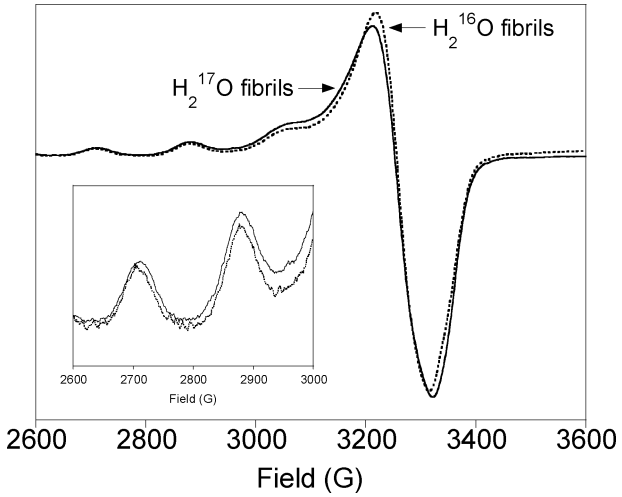

FIGURE 5: 10 K EPR spectra of Aβ40 fibrils containing Cu^{2+} assembled in $H_2{}^{16}O$ (dashed line) or 35−40% enriched $H_2{}^{17}O$ (solid line). The spectrum for the sample in $H_2{}^{16}O$ was increased by a factor of 2 to facilitate line shape comparison. EPR parameters: microwave frequency = 9.386, microwave power = 0.5 mW, modulation amplitude = 10 G, time constant = 40.96 ms, conversion time = 40.96 ms, gain = 5×10^4, eight scans. Sample preparation protocol is in Materials and Methods.

solution was saved and an EPR spectrum was collected to show that it contains mostly free Cu^{2+} (Figure 4, spectrum b). The fibrils were then washed with buffer containing Tris, centrifuged to pellet the fibrils, and resuspended in the same buffer. EPR spectra were collected of the wash solution (Figure 4, spectrum a) and the Cu^{2+}-containing Aβ40 fibrils (Figure 4, spectrum c). The spectra show that Cu^{2+} bound to Aβ40 fibrils assembled in the presence of excess Cu^{2+} cannot be removed by washing fibrils with Tris buffer, a weak chelator of Cu^{2+} (log $K_{app} = 1.8$ (*10*)), suggesting that Cu^{2+} is not bound loosely to the exterior of fibrils. The wash solution contains a small amount of Cu^{2+}, bound either to soluble Aβ40 monomer or to Aβ40 oligomers that do not

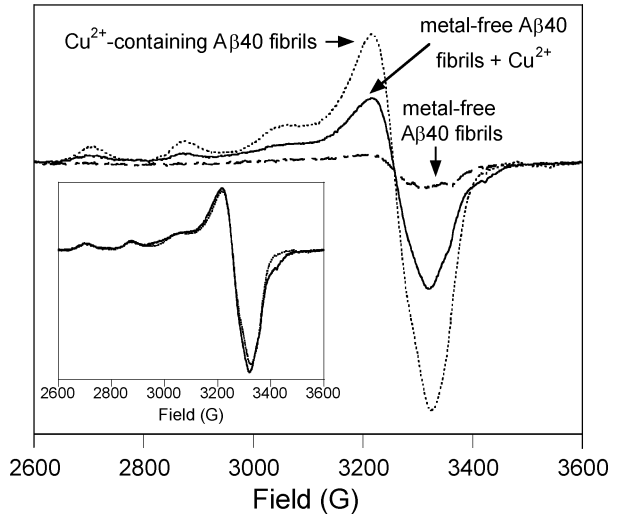

FIGURE 6: 20 K EPR spectra of Aβ40 fibrils assembled with Cu^{2+} (Cu^{2+}-containing Aβ40 fibrils, dashed line) or without Cu^{2+} (metal-free Aβ40 fibrils, double-dashed line). After collection of an initial metal-free Aβ40 fibrils spectrum, 43 μM Cu^{2+} was added to Aβ40 fibrils (metal-free Aβ40 fibrils + Cu^{2+}, solid line). The spectrum shown was collected after 30 min room temperature incubation of the sample. The Aβ40 fibrils containing Cu^{2+} were isolated from a solution of 100 μM Aβ40 containing 100 μM Cu^{2+}; Aβ40 fibrils without Cu^{2+} were isolated from a solution of 100 μM Aβ40. Both samples were in 50 mM NaPi, 75 mM NaCl, pH 7.2 buffer containing 50% glycerol (v/v). The inset shows that the spectral shape for Cu^{2+}-containing Aβ40 fibrils is the same as that for metal-free Aβ40 fibrils to which Cu^{2+} was added. EPR parameters: microwave frequency = 9.386, microwave power = 0.5 mW, modulation amplitude = 10 G, time constant = 40.96 ms, conversion time = 40.96 ms, gain = 5×10^4, eight scans.

precipitate upon centrifugation. Tris buffer was used in these experiments because Cu^{2+} in Tris buffer displays an EPR signal distinct from that for Cu^{2+} bound to Aβ (Figure 4, spectrum d). Fibrils were not detected by ThT assay in the supernatant or wash solutions separated from Aβ40 fibrils assembled in the presence of excess Cu^{2+} (Supporting Information Figure S6). This experiment shows that Cu^{2+} is not nonspecifically bound to the surface of fibrils, but instead is incorporated in a well-defined binding site on the fibrils.

Substitution of $H_2{}^{17}O$ for $H_2{}^{16}O$ can reveal if water is in the coordination sphere of Cu^{2+} in Aβ because the Cu^{2+} hyperfine lines broaden when ^{17}O is bound to Cu^{2+} (*54*, *55*). Thus, the Cu^{2+} EPR signal will change if water is an equatorial ligand to Cu^{2+} in Aβ. When water molecules are axial ligands to type 2 Cu^{2+} ions, spectral broadening is not observed because coupling between axial ligand donor atoms and the unpaired electron in the $d_{x^2-y^2}$ orbital on Cu^{2+} is weak. There are two situations in which water might be an equatorial ligand to Cu^{2+}. The first is if Cu^{2+} is bound to the outside of fibrils. The second is if water replaces a ligand to Cu^{2+} upon Y10 mutation, as proposed for Aβ42Y10A (*30*). To test whether water is a ligand to Cu^{2+} in fibrils, Aβ40 fibrils were assembled in the presence of Cu^{2+} and $H_2{}^{16}O$ or $H_2{}^{17}O$ (*54*, *55*). Minimal broadening of the Cu^{2+} peaks is observed in $H_2{}^{17}O$ (Figure 5), showing that water is not in the equatorial coordination sphere of Cu^{2+} (*54*, *55*). Based on results for laccase, the expected hyperfine coupling constant for $H_2{}^{17}O$ bound to a type 2 copper site is 11−12 G, which causes a 20 G increase in the peak width at half-height (*54*, *55*). The widths at half-height for the Cu^{2+} hyperfine peaks in $H_2{}^{16}O$ are 54 ± 7 G ($m_I = -3/2$), 54 ± 5

G ($m_I = -1/2$). In $H_2{}^{17}O$, the widths at half-height for the same peaks are 59 ± 4 G and 58 ± 3 G, respectively. For Aβ16Y10F, spectra in $H_2{}^{17}O$ and $H_2{}^{16}O$ are identical (Figure S7, Supporting Information), indicating that water is not a ligand to Cu^{2+} in Aβ tyrosine mutants either.

If Cu^{2+} is a key constituent of fibril nuclei, as has been proposed for Zn^{2+} (*15*), fibrils assembled in the *absence* of Cu^{2+} might not bind exogenous Cu^{2+}, or might bind it in a different environment from fibrils initially assembled in the *presence* of Cu^{2+}. We find that fibrils assembled without Cu^{2+} can bind added Cu^{2+} to give an EPR spectrum similar to that observed for fibrils initially assembled in the presence of Cu^{2+} (Figure 6). The EPR parameters ($g_{||} = 2.265$; $A_{||} = 172 \pm 2$ G) are the same as for Cu^{2+} bound to soluble Aβ40 (Table 2) or for fibrils of Aβ40 assembled in the presence of Cu^{2+} (*31*). The Cu^{2+} EPR spectrum obtained immediately after mixing (1 min) and that collected after incubation of the sample at room temperature for 30 min are the same (1 min spectrum not shown). In phosphate buffers, Cu^{2+} binding to Aβ can be monitored directly by EPR as a function of time because free Cu^{2+} produces weak (or no) hyperfine lines while Cu^{2+} bound to Aβ gives large hyperfine peaks. Because no decrease in the doubly integrated Cu^{2+} EPR signal intensity is observed as a function of room temperature incubation time, Cu^{2+} is not reduced to Cu^{1+} by Aβ40 in fibrils, a reaction that has been reported for Cu^{2+} bound to soluble Aβ40 (*20*−*23*, *30*). Moreover, these results indicate that metal-free Aβ40 fibrils can incorporate Cu^{2+} into a binding site on Aβ *after* fibril formation.

DISCUSSION

Relative metal ion affinity for proteins and peptides can be determined by monitoring changes in tyrosine and/or tryptophan fluorescence intensity and fitting the data to an appropriate binding model. When measured in this manner, the apparent affinity of Cu^{2+} for the Aβ peptides in Table 1 is in the order Aβ4-16 > Aβ40 > Aβ28 > Aβ16; all of the apparent dissociation constants are in the micromolar range. By tyrosine fluorescence, high affinity sites were not detected in this work (*14*) because of the presence of Tris, a weak ligand to Cu^{2+} (*10*). Previous results indicate micromolar (*14*), nanomolar (*33*), or attomolar affinities of Cu^{2+} for Aβ (*10*, *17*), depending on the conditions under which the experiments were performed. Kowalik-Jankowska et al. (*13*, *32*) have reported increasing stability constants at pH 7 for the Cu^{2+} complexes formed with Aβ peptides of increasing length (Aβ10, log $\beta = 3.60$; Aβ16, log $\beta = 20.12$; Aβ28, log $\beta = 31.58$). We also observe an increase in the apparent affinity of Cu^{2+} for Aβ as the peptide length increases. Our apparent dissociation constants are conditional, and we used them only to discern the effect of a change in peptide sequence on Cu^{2+} affinity in our buffers.

One of the important unresolved questions regarding the Cu^{2+} coordination environment in Aβ is the identity of the metal ion ligating groups. Possible ligands in Aβ for Cu^{2+} are histidine (H6, H13, H14), tyrosine (Y10), aspartate or glutamate (D1, E3, D7, E11, E22, D23), methionine (M35), deprotonated amides of the peptide backbone, or carbonyl groups (*9*, *11*, *12*, *15*, *35*). While not all of these residues are at the N-terminus of Aβ, which is where Cu^{2+} is proposed to bind, these groups are common ligands for Cu^{2+} in peptides (*12*, *13*, *44*, *56*) and proteins (*57*). Our $g_{||}$ and $A_{||}$ values for Cu^{2+} bound to soluble Aβ16, Aβ16Y10F, Aβ28, Aβ40, and Aβ42 are most consistent with 3N1O coordination at pH ≈ 7 (*13*, *17*, *32*, *33*, *53*). Based on a 3N1O coordination environment, the binding site for Cu^{2+} on Aβ has been proposed to consist of the three histidines H6, H13, and H14, and tyrosine Y10 (*10*, *11*, *22*, *23*, *29*, *30*, *58*). When we used the peptides Aβ4-16 or Aβ2-16, which contain H6, Y10, H13, and H14, the Cu^{2+} coordination environment and the apparent dissociation constants are very different from those observed for the native peptide. These differences raise the possibility that deletions at the N-terminus affect the thermodynamic landscape to such an extent that the 3 His/1 Tyr coordination sphere is no longer the energetic minimum. However, it is also possible that the coordination environment of Cu^{2+} in native Aβ is not composed exclusively of histidines and tyrosine.

Consistent with previous work (*11*−*13*, *20*, *29*, *30*, *33*), we find that Cu^{2+} is coordinated to a ligand via an oxygen atom in soluble Aβ at pH 7.2−7.4. Our results confirm the work of others showing that tyrosine is not the O-atom donor ligand to Cu^{2+} (*32*, *33*). We find that Aβ tyrosine fluorescence is not quenched entirely in the presence of $Cu^{2+}$and that EPR spectra of Cu^{2+} bound to a Y10F mutant are identical to those collected for Cu^{2+} bound to the native peptide. If Cu^{2+} is bound directly to the phenolate oxygen of tyrosine, Cu^{2+} should exert intersystem crossing effects due to a contact interaction and quench tyrosine fluorescence dramatically (*50*). Garzon-Rodriguez et al. observed a similar lack of complete fluorescence quenching for Cu^{2+} bound to Aβ40 and Aβ42, with end-of-titration fluorescence intensities of 53% and 26%, respectively. Tyrosinate is not the O-atom donor ligand to Cu^{2+} because the tyrosine fluorescence wavelength maximum does not red shift in the presence of Cu^{2+} (*50*). Consistent with these findings are Raman measurements on senile plaque cores containing Aβ and Cu^{2+} (*9*) that show no evidence for tyrosinate coordination to Cu^{2+}. Kowalik-Jankowska et al. have shown that the pK_a of Y10 in Aβ16 and Aβ28 does not change in the presence of Cu^{2+} (*32*). Syme et al. have demonstrated that tyrosine ^{1}H chemical shifts in Aβ28 are unaffected by the addition of Cu^{2+} (*33*). Further evidence against Y10 coordination to Cu^{2+} is from EPR spectra of Cu^{2+} bound to rat Aβ28 (*11*), which reportedly binds Cu^{2+} in a 2N2O coordination environment, even though rat Aβ does not contain Y10. Taken together, the most reasonable conclusion is that Y10 is not the O-atom donor ligand to Cu^{2+} in native Aβ.

Recently, Barnham et al. (*30*) proposed tyrosine coordination to Cu^{2+} based on a shift in $g_{||}$ in the EPR spectrum of Cu^{2+} bound to Aβ42Y10A. Like the Y10F mutant used here, Cu^{2+} was found to be bound to Aβ42Y10A in a 3N1O coordination environment (*30*). To explain the identical coordination environment for Cu^{2+} in Aβ42Y10F and Aβ42, the authors suggest that water, phosphate, or another O-atom donor ligand substitutes for tyrosine in the mutant. We have shown that water is not a ligand to Cu^{2+} in AβY10F by substituting $H_2{}^{17}O$ for $H_2{}^{16}O$. Our results do not rule out phosphate or another O-atom donor ligand to Cu^{2+} in Y10 mutants; however, we believe the small change in $g_{||}$ observed by Barnham et al. more likely is due to a change in geometry at the metal ion rather than loss of tyrosine in the coordination sphere of Cu^{2+} in Aβ42Y10A (*30*).

Deletion of N-terminal amino acids, including D1, a proposed ligand to Cu^{2+} in Aβ16 or Aβ28 at pH 7 (*32*, *33*), shows that the coordination environment of Cu^{2+} bound to Aβ is sensitive to such changes, consistent with work on other metal-binding sites in Cu^{2+}−peptide systems (*56*, *59*). Our findings that the Cu^{2+} coordination environment is different in Aβ16, Aβ2-16, and Aβ4-16 further establish the importance of the amino terminus in binding Cu^{2+}. Other work has shown that acetylation of the N-terminus of Aβ16 changes the type of N-donors to Cu^{2+} from two histidines and the amino terminus to three histidines (*32*). Circular dichroism spectroscopy of N-terminal acetylated Aβ28 similarly implicates the amino terminus and histidines in Cu^{2+} binding (*33*). Although the N-terminal truncated peptides used here are not physiologically relevant, they illustrate the importance of the N-terminus in creating the binding site for Cu^{2+} in native Aβ.

If one of the N-atom donors to Cu^{2+} in native Aβ is the amino terminus, two other N-atom donors remain to be identified. Potentiometric titrations of soluble Aβ16 and Aβ28 support coordination of H13 and H14 to Cu^{2+} (*32*), and other spectroscopic measurements indicate that at least two histidines (or up to three, depending on pH) in Aβ are bound to Cu^{2+} (*33*). We propose H6 and H13 as the two histidines bound to Cu^{2+} in Aβ because the EPR spectrum of Cu^{2+} bound to soluble Aβ is nearly identical to that observed for Cu^{2+} bound to Aβ40 fibrils. Solid state NMR measurements of Aβ fibrils have shown that both H13 and H14 are in a region of Aβ expected to be in β-strands (*34*, *60*−*67*). Such an arrangement forces H13 and H14 to be on opposite sides of β-sheets in fibrils (*15*), precluding ligation of both histidines in a single peptide to the same Cu^{2+} ion if fibrils assembled in the presence of Cu^{2+} adopt a parallel β-sheet structure. Because metal-free Aβ40 fibrils can bind Cu^{2+} to produce an EPR spectrum like that for Cu^{2+}-containing fibrils, H13 and H14 in a single peptide probably do not both ligate Cu^{2+} in Aβ fibrils, because β-sheets would be disrupted. If Cu^{2+} is ligated exclusively to H13 and H14 residues derived from *multiple* peptides, as proposed for Zn^{2+} in fibrils (*15*, *34*), EPR spectra of Cu^{2+} in fibrils should show four N-donor atom ligands to Cu^{2+}. Our results showing a Cu^{2+} coordination environment in Aβ fibrils of 3N1O and a stoichiometry of one Cu^{2+} ion per peptide (*31*) seem to rule out Cu^{2+} cross-linking β-sheets in fibrils via four histidines from multiple peptides.

Metal ions can be removed from Aβ plaques with a chelator causing the plaques to "loosen" (*9*) and disaggregate (*28*). A variety of chelators has been used to remove metal ions from Aβ aggregates including clioquinol, TPEN, EGTA, and EDTA (*9*, *10*, *27*, *28*). Because these chelators bind Cu^{2+} very tightly, such experiments cannot indicate whether Cu^{2+} is associated with the exterior surface, where Cu^{2+} might be weakly bound, or in the interior of aggregates, where Cu^{2+} might be bound more strongly. We find that fibrils assembled with Cu^{2+} and washed with buffer retain Cu^{2+}, indicating that Cu^{2+} is not removed easily from the fibrils. If Cu^{2+} is bound to the exterior of fibrils, water might be in the equatorial coordination sphere of Cu^{2+}. We tested this hypothesis by assembling fibrils in either $H_2{}^{16}O$ or $H_2{}^{17}O$. No significant broadening of the Cu^{2+} EPR signal was observed confirming that water is not the O-atom donor ligand to Cu^{2+} in fibrils. Together, these results indicate that Cu^{2+} is located in the fibrils and bound to ligands derived from Aβ rather than solvent.

Because Cu^{2+} is not *necessary* for Aβ fibril formation, as shown here by Cu^{2+} incorporation into metal-free fibrils, it might not have a direct catalytic role in fibrillogenesis. In other words, Cu^{2+} might not participate intimately in β-sheet formation via alteration of the Cu^{2+} coordination sphere (*11*). Yoshiike et al. (*19*) and Zou et al. (*16*) have demonstrated that Cu^{2+} inhibits Aβ β-sheet formation. These results contradict our TEM results showing that fibrils form in the presence of Cu^{2+} and that these fibrils contain Cu^{2+} (*31*). All of these data can be reconciled by a model in which Cu^{2+} can bind to fibrils at any point during fibrillization because it binds to an N-terminal segment of Aβ that is *not* involved in β-sheet formation. A binding site for Cu^{2+} that includes the N-terminus (*13*, *32*, *33*) would not destabilize β-sheets in the interior of the fibrils and would explain why the binding site for Cu^{2+} is sensitive to N-terminal acetylation (*13*, *32*, *33*) or deletion of D1, A2, and E3. This model for Cu^{2+} binding to Aβ is consistent with studies showing that the N-terminal region of the peptide is not confined rigidly in mature fibrils assembled without Cu^{2+} (*68*−*73*), that the first nine amino acids are not required for fibril formation (*66*, *74*, *75*), and that a Cu^{2+}-binding site in Aβ40 is located near the N-terminus (*11*, *12*, *20*, *76*). Our proposal for the native Cu^{2+} binding site at physiological pH includes the amino terminus, a carboxylate from D1 or E3, and histidines (H6 and H13) within the first sixteen amino acids of Aβ.

ACKNOWLEDGMENT

We would like to acknowledge critical reading of the manuscript by Dr. David H. Stewart and helpful discussions with Dr. Donald J. Creighton, Dr. Ralph M. Pollack, and Dr. Colin Garvie. The expertise of Dr. R. Nauman of the UMB-Dental School Microscopy Facility in obtaining TEM images is appreciated also.

SUPPORTING INFORMATION AVAILABLE

Uncorrected tyrosine fluorescence titration data, thioflavin T fluorescence data, temperature dependences of EPR spectra for soluble Aβ28 and Aβ40 fibrils containing Cu^{2+}, and EPR spectra of Aβ16Y10F with Cu^{2+} in $H_2{}^{16}O$ or $H_2{}^{17}O$ buffers. This material is available free of charge via the Internet at http://pubs.acs.org.

REFERENCES

1. Moir, R. D., Atwood, C. S., Huang, X., Tanzi, R. E., and Bush, A. I. (1999) Mounting evidence for the involvement of zinc and copper in Alzheimer's disease, *Eur. J. Clin. Invest. 29*, 569−570.
2. Bush, A. I., Multhaup, G., Moir, R. D., Williamson, T. G., Small, D. H., Rumble, B., Pollwein, P., Beyreuther, K., and Masters, C. L. (1993) A Novel Zinc(II) Binding Site Modulates the Function of the βA4 Amyloid Protein Precursor of Alzheimer's Disease, *J. Biol. Chem. 268*, 16109−16112.
3. Bush, A. I., Pettingell, W. H., Multhaup, G., Paradis, M. D., Vonsattel, J. P., Gusella, J. F., Beyreuther, K., Masters, C. L., and Tanzi, R. E. (1994) Rapid Induction of Alzheimer Aβ Amyloid Formation by Zinc, *Science 265*, 1464−1467.
4. Rottkamp, C. A., Raina, A. K., Zhu, X., Gaier, E., Bush, A. I., Atwood, C. S., Chevion, M., Perry, G., and Smith, M. A. (2001) Redox-Active Iron Mediates Amyloid-β Toxicity, *Free Radical Biol. Med. 30*, 447−450.
5. Jacobson, D. R., and Buxbaum, J. N. (1991) Genetic Aspects of Amyloidosis, *Adv. Hum. Genet. 20*, 69−123.

6. Pepys, M. B. (1998) Amyloidosis, in *Immunological Diseases* (Samter, M., Ed.) pp 631−674, Little, Brown and Company, Boston.
7. Sipe, J. D. (1992) Amyloidosis, *Annu. Rev. Biochem. 61*, 947−975.
8. Beauchemin, D., and Kisilevsky, R. (1998) A Method Based on ICP-MS for the Analysis of Alzheimer's Amyloid Plaques, *Anal. Chem. 70*, 1026−1029.
9. Dong, J., Atwood, C. G., Anderson, V. E., Siedlak, S. L., Smith, M. A., Perry, G., and Carey, P. R. (2003) Metal Binding and Oxidation of Amyloid-β within Isolated Senile Plaque Cores: Raman Microscopic Evidence, *Biochemistry 42*, 2768−2773.
10. Atwood, C. S., Scarpa, R. C., Huang, X., Moir, R. D., Jones, W. D., Fairlie, D. P., Tanzi, R. E., and Bush, A. I. (2000) Characterization of Copper Interactions with Alzheimer Amyloid β Peptides: Identification of an Attomolar-Affinity Copper Binding Site on Amyloid β1-42, *J. Neurochem. 75*, 1219−1233.
11. Curtain, C. C., Ali, F., Volitakis, I., Cherny, R. A., Norton, R. S., Beyreuther, K., Barrow, C. J., Masters, C. L., Bush, A. I., and Barnham, K. J. (2001) Alzheimer's Disease Amyloid-β Binds Copper and Zinc to Generate and Allosterically Ordered Membrane-penetrating Structure Containing Superoxide Dismutase-like Subunits, *J. Biol. Chem. 276*, 20466−20473.
12. Miura, T., Suzuki, K., Kohata, N., and Takeuchi, H. (2000) Metal Binding Modes of Alzheimer's Amyloid β-Peptide in Insoluble Aggregates and Soluble Complexes, *Biochemistry 39*, 7024−7031.
13. Kowalik-Jankowska, T., Dolejsz-Ruta, M., Wisniewska, K., and Lankiewicz, L. (2001) Cu(II) interaction with N-terminal fragments of human and mouse β-amyloid peptide, *J. Inorg. Biochem. 86*, 535−545.
14. Garzon-Rodriguez, W., Yatsimirsky, A. K., and Glabe, C. G. (1999) Binding of Zn(II), Cu(II), and Fe(II) Ions to Alzheimer's Aβ Peptide Studied by Fluorescence, *Bioorg. Med. Chem. Lett. 9*, 2243−2248.
15. Morgan, D. M., Dong, J., Jacob, J., Lu, K., Apkarian, R. P., Thiyagarajan, P., and Lynn, D. G. (2002) Metal Switch for Amyloid Formation: Insight into the Structure of the Nucleus, *J. Am. Chem. Soc. 124*, 12544−12645.
16. Zou, J., Kajita, K., and Sugimoto, N. (2001) Cu^{2+} Inhibits the Aggregation of Amyloid β-Peptide(1-42) in vitro, *Angew. Chem., Int. Ed. 40*, 2274−2277.
17. Atwood, C. S., Moir, R. D., Huang, X., Scarpa, R. C., Bacarra, N. M. E., Romano, D. M., Hartshorn, M. A., Tanzi, R. E., and Bush, A. I. (1998) Dramatic Aggregation of Alzheimer Aβ by Cu(II) is Induced by Conditions Representing Physiological Acidosis, *J. Biol. Chem. 273*, 12817−12826.
18. Cuajungco, M. P., Goldstein, L. E., Nunomura, K., Smith, M. A., Lim, J. T., Atwood, C. S., Huang, X., Farrag, Y. W., Perry, G., and Bush, A. I. (2000) Evidence that the β-Amyloid Plaques of Alzheimer's Disease Represent the Redox-silencing and Entombment of Aβ by Zinc, *J. Biol. Chem. 275*, 19439−19442.
19. Yoshiike, Y., Tanemura, K., Murayama, O., Akagi, T., Murayama, M., Sato, S., Sun, X., Tanaka, N., and Takashima, A. (2001) New Insights on How Metals Disrupt Amyloid β-Aggregation and Their Effects on Amyloid-β Cytotoxicity, *J. Biol. Chem. 276*, 32293−32299.
20. Huang, X., Cuajungco, M. P., Atwood, C. G., Hartshorn, M. A., Tyndall, J. D. A., Hanson, G. R., Stokes, K. C., Leopold, M., Multhaup, G., Goldstein, L. E., Scarpa, R. C., Saunders, A. J., Lim, J., Moir, R. D., Glabe, C., Bowden, E. F., Masters, C. L., Fairlie, D. P., Tanzi, R. E., and Bush, A. I. (1999) Cu(II) Potentiation of Alzheimer Aβ Neurotoxicity, *J. Biol. Chem. 274*, 37111−37116.
21. Huang, X., Atwood, C. G., Hartshorn, M. A., Multhaup, G., Goldstein, L. E., Scarpa, R. C., Cuajungco, M. P., Gray, D. N., Lim, J., Moir, R. D., Tanzi, R. E., and Bush, A. I. (1999) The Aβ Peptide of Alzheimer's Disease Directly Produces Hydrogen Peroxide through Metal Ion Reduction, *Biochemistry 38*, 7609−7616.
22. Barnham, K. J., Ciccotosto, G. D., Tickler, A. K., Ali, F. E., Smith, D. G., Williamson, N. A., Lam, Y.-H., Carrington, D., Tew, D., Kocak, G., Volitakis, I., Separovic, F., Barrow, C. J., Wade, J. D., Masters, C. L., Cherny, R. A., Curtain, C. C., Bush, A. I., and Cappai, R. (2003) Neurotoxic, Redox-competent Alzheimer's β-Amyloid is Released from Lipid Membrane by Methionine Oxidation, *J. Biol. Chem. 278*, 42959−42965.
23. Opazo, C., Huang, X., Cherny, R. A., Moir, R. D., Roher, A. E., White, A. R., Cappai, R., Masters, C. L., Tanzi, R. E., Inestrosa, N. C., and Bush, A. I. (2002) Metalloenzyme-like Activity of Alzheimer's Disease β-Amyloid, *J. Biol. Chem. 43*, 40302−40308.
24. Kirkitadze, M. D., Bitan, G., and Teplow, D. B. (2002) Paradigm shifts in Alzheimer's disease and other neurodegenerative disorders: the emerging role of oligomeric assemblies, *J. Neurosci. Res. 69*, 567−577.
25. Bush, A. I. (2002) Metal Complexing agents and therapies for Alzheimer's disease, *Neurobiol. Aging 23*, 1031−1038.
26. Ritchie, C. W., Bush, A. I., MacKinnon, A., Macfarlane, S., Mastwyk, M., MacGregor, L., Kiers, L., Cherny, R. A., Li, Q.-X., Tammer, A., Carrington, D., Mavros, C., Volitakis, I., Xilinas, M. E., Armes, D., Davis, S., Beyreuther, K., Tanzi, R. E., and Masters, C. L. (2003) Metal-Protein Attenuation with Iodochlorhydroxyquin (Clioquinol) Targeting Aβ Amyloid Deposition and Toxicity in Alzheimer Disease, *Arch. Neurol. 60*, 1675−1677.
27. Cherny, R. A., Atwood, C. S., Xilinas, M. E., Gray, D. N., Jones, W. D., McLean, C. A., Barnham, K. J., Volitakis, I., Fraser, F. W., Kim, Y.-S., Huang, X., Goldstein, L. E., Moir, R. D., Lim, J. T., Beyreuther, K., Zheng, H., Tanzi, R. E., Masters, C. L., and Bush, A. I. (2001) Treatment with a Copper−Zinc Chelator Markedly and Rapidly Inhibits β-Amyloid Accumulation in Alzheimer's Disease Transgenic Mice, *Neuron 30*, 665−676.
28. Cherny, R. A., Legg, J. T., McLean, C. A., Fairlie, D. P., Huang, X., Atwood, C. S., Beyreuther, K., Tanzi, R. E., Masters, C. L., and Bush, A. I. (1999) Aqueous Dissolution of Alzheimer's Disease in Aβ Amyloid Deposits by Biometal Depletion, *J. Biol. Chem. 274*, 23223−23228.
29. Curtain, C. C., Ali, F. E., Smith, D. G., Bush, A. I., Masters, C. L., and Barnham, K. J. (2003) Metal Ions, pH, and Cholesterol Regulate the Interactions of Alzheimer's Disease Amyloid-b peptide with membrane lipid, *J. Biol. Chem. 278*, 2977−2982.
30. Barnham, K. J., Haeffner, F., Ciccotosto, G. D., Curtain, C. C., Tew, D., Mavros, C., Beyreuther, K., Carrington, D., Masters, C. L., Cherny, R. A., Cappai, R., and Bush, A. I. (2004) Tyrosine Gated electron transfer is the key to the toxic mechanism of Alzheimer's Disease β-amyloid, *FASEB J. 18*, 1427−1429.
31. Karr, J. W., Kaupp, L. J., and Szalai, V. A. (2004) Amyloid-β binds Cu(II) in a Mononuclear Metal Ion Binding Site, *J. Am. Chem. Soc. 126*, 13534−13538.
32. Kowalik-Jankowska, T., Ruta, M., Wisniewska, K., and Lankiewicz, L. (2003) Coordination abilities of the 1-16 and 1-28 fragments of β-amyloid peptide towards copper(II) ions: a combined potentiometric and spectroscopic study, *J. Inorg. Biochem. 95*, 270−282.
33. Syme, C. D., Nadal, R. C., Rigby, S. E. J., and Viles, J. H. (2004) Copper Binding to the Amyloid-β (Aβ) Peptide Associated with Alzheimer's Disease: FOLDING, COORDINATION GEOMETRY, pH DEPENDENCE, STOICHIOMETRY, AND AFFINITY OF Aβ-(1-28): INSIGHTS FROM A RANGE OF COMPLEMENTARY SPECTROSCOPIC TECHNIQUES, *J. Biol. Chem. 279*, 18169−18177.
34. Lynn, D. G., and Meredith, S. C. (2000) Review: Model Peptides and the Physicochemical Approach to β-Amyloids, *J. Struct. Biol. 130*, 153−173.
35. Liu, S.-T., Howlett, G., and Barrow, C. J. (1999) Histidine-13 is a Crucial Residue in the Zinc Ion-Induced Aggregation of the Aβ Peptide of Alzheimer's Disease, *Biochemistry 38*, 9373−9378.
36. Wood, S. J., Maleeff, B., Hart, T., and Wetzel, R. (1996) Physical, Morphological and Functional Differences between pH 5.8 and 7.4 Aggregates of the Alzheimer's Amyloid Peptide Aβ, *J. Mol. Biol. 256*, 870−877.
37. Zagorski, M. G., Yang, J., Shao, H., Ma, K., Zeng, H., and Hong, A. (1999) Methodological and Chemical Factors Affecting Amyloid β Peptide Amyloidogenicity, *Methods Enzymol. 309*, 189−204.
38. Stine, W. B., Jr., Dahlgren, K. N., Krafft, G. A., and LaDu, M. J. (2003) In vitro characterization of conditions for amyloid-beta peptide oligomerization and fibrillogenesis, *J. Biol. Chem. 278*, 11612−11622.
39. Balbach, J. J., Ishii, Y., Antzutkin, O. N., Leapman, R. D., Rizzo, N. W., Dyda, F., Reed, J., and Tycko, R. (2000) Amyloid Fibril Formation by Aβ_{16-22}, a Seven-Residue Fragment of the Alzheimer's β-Amyloid Peptide, and Structural Characterization by Solid State NMR, *Biochemistry 39*, 13748−13759.
40. Tjernberg, L. O., Näslund, J., Lindqvist, F., Johansson, J., Karlström, A. R., Thyberg, J., Terenius, L., and Nordstedt, C. (1996) Arrest of β-Amyloid Fibril Formation by a Pentapeptide Ligand, *J. Biol. Chem. 271*, 8545−8548.

41. Tjernberg, L. O., Pramanik, A., Bjorling, S., Thyberg, P., Thyberg, J., Nordstedt, C., Berndt, K. D., Terenius, L., and Rigler, R. (1999) Amyloid β-peptide polymerization studied using fluorescence correlation spectroscopy, *Chem. Biol. 6*, 53−62.
42. Findeis, M. A., Musso, G. M., Arico-Muendel, C. C., Benjamin, H. W., Hundal, A. M., Lee, J.-J., Chin, J., Kelley, M., Wakefield, J., Hayward, N. J., and Molineaux, S. M. (1999) Modified-Peptide Inhibitors of Amyloid β-Peptide Polymerization, *Biochemistry 38*, 6791−6800.
43. Lowe, T. L., Strzelec, A., Kiessling, L. L., and Murphy, R. M. (2001) Structure−Function Relationships for Inhibitors of β-Amyloid Toxicity Containing the Recognition Sequence KLVFF, *Biochemistry 40*, 7882−7889.
44. Aronoff-Spencer, E., Burns, C. S., Avdievich, N. I., Gerfen, G. J., Peisach, J., Antholine, W. E., Ball, H. L., Cohen, F. E., Prusiner, S. B., and Millhauser, G. L. (2000) Identification of the Cu^{2+} Binding Sites in the N−Terminal Domain of the Prion Protein by EPR and CD Spectroscopy, *Biochemistry 39*, 13760−13771.
45. Wertz, J. E., and Bolton, J. R. (1972) *Electron Spin Resonance: Elementary Theory and Practical Applications*, Chapman & Hall, New York.
46. Levine, H. I. (1999) *Methods Enzymol. 309*, 274−284.
47. Moffett, J., Zika, R. G., and Petasne, R. G. (1985) Evaluation of Bathocuproine for the Spectrophotometric Determination of Copper(I) in Copper Redox Studies with Applications in Studies of Natural Waters, *Anal. Chim. Acta 175*, 171−179.
48. Harper, J. D., Wong, S. S., Lieber, C. M., and Lansbury, P. T., Jr. (1999) Assembly of Aβ Amyloid Protofibrils: An in Vitro Model for a Possible Early Event in Alzheimer's Disease, *Biochemistry 38*, 8972−8980.
49. Tycko, R. (2004) Progress towards a molecular-level structural understanding of amyloid fibrils, *Curr. Opin. Struct. Biol. 14*, 96−103.
50. Lakowicz, J. R. (1999) *Principles of Fluorescence*, 2nd ed., Kluwer Academic/Plenum, New York.
51. Huang, C. Y. (1982) Determination of Binding Stoichiometry by the Continuous Variation Method: The Job Plot, *Methods Enzymol. 87*, 509−525.
52. Creighton, T. E. (1993) *Proteins: Structures and Molecular Properties*, 2nd ed., Freeman and Company, New York.
53. Peisach, J., and Blumberg, W. E. (1974) Structural Implications Derived from the Analysis of Electron Paramagnetic Resonance Spectra of Natural and Artificial Copper Proteins, *Arch. Biochem. Biophys. 165*, 691−708.
54. Brändén, R., and Deinum, J. (1977) Type 2 Copper(II) as a component of the dioxygen reducing site in laccase: evidence from EPR experiments with ^{17}O, *FEBS Lett. 73*, 144−146.
55. Deinum, J. S. E., and Vänngård, T. (1975) ^{17}O Hyperfine Interaction in the EPR Spectrum of Fungal Laccase A, *FEBS Lett. 58*, 62−65.
56. Sigel, H., and Martin, B. R. (1982) Coordinating Properties of the Amide Bond. Stability and Structure of Metal Ion Complexes of Peptides and Related Ligands, *Chem. Rev. 82*, 385−426.
57. Holm, R. H., Kennepohl, P., and Solomon, E. I. (1996) Structural and Functional Aspects of Metal Sites in Biology, *Chem. Rev. 96*, 2239−2314.
58. Atwood, C. G., Perry, G., Zeng, H., Kato, Y., Jones, W. D., Ling, K.-Q., Huang, X., Moir, R. D., Wang, D., Sayre, L. M., Smith, M. A., Chen, S. G., and Bush, A. I. (2004) Copper Mediates Dityrosine Cross-Linking of Alzheimer's Amyloid-β, *Biochemistry 43*, 560−568.
59. Martin, B. R., and Edsall, J. T. (1960) The Association of Divalent Cations with Acylated Histidine Derivatives, *J. Am. Chem. Soc. 82*, 1107−1111.
60. Tycko, R., and Ishii, Y. (2003) Constraints on supramolecular structure in amyloid fibrils from two-dimensional solid-state NMR spectroscopy with uniform isotopic labeling, *J. Am. Chem. Soc. 125*, 6606−6607.
61. Tycko, R. (2003) Insights into the amyloid folding problem from solid-state NMR, *Biochemistry 42*, 3151−3159.
62. Antzutkin, O. N., Leapman, R. D., Balbach, J. J., and Tycko, R. (2002) Supramolecular structural constraints on Alzheimer's beta-amyloid fibrils from electron microscopy and solid-state nuclear magnetic resonance, *Biochemistry 41*, 15436−15450.
63. Petkova, A. T., Ishii, Y., Balbach, J. J., Antzutkin, O. N., Leapman, R. D., Delaglio, F., and Tycko, R. (2002) A structural model for Alzheimer's beta-amyloid fibrils based on experimental constraints from solid state NMR, *Proc. Natl. Acad. Sci. U.S.A. 99*, 16742−16747.
64. Balbach, J. J., Petkova, A. T., Oyler, N. A., Antzutkin, O. N., Gordon, D. J., Meredith, S. C., and Tycko, R. (2002) Supramolecular Structure in Full-Length Alzheimer's β-Amyloid Fibrils: Evidence for a Parallel β-Sheet Organization from Solid State Nuclear Magnetic Resonance, *Biophys. J. 83*, 1205−1216.
65. Burkoth, T. S., Benzinger, T. L. S., Urban, V., Morgan, D. M., Gregory, D. M., Thiyagarajan, P., Botto, R. E., Meredith, S. C., and Lynn, D. G. (2000) Structure of the β-Amyloid$_{(10-35)}$ Fibril, *J. Am. Chem. Soc. 122*, 7883−7889.
66. Benzinger, T. L. S., Gregory, D. M., Burkoth, T. S., Miller-Auer, H., Lynn, D. G., Botto, R. E., and Meredith, S. C. (1998) Propagating Structure of Alzheimer's β-Amyloid$_{(10-35)}$ is Parallel β-Sheet with Residues in Exact Register, *Proc. Natl. Acad. Sci. U.S.A. 95*, 13407−13412.
67. Benzinger, T. L. S., Gregory, D. M., Burkoth, T. S., Miller-Auer, H., Lynn, D. G., Botto, R. E., and Meredith, S. C. (2000) Two-Dimensional Structure of β-Amyloid$_{(10-35)}$ Fibrils, *Biochemistry 39*, 3491−3499.
68. Iwata, K., Eyles, S. J., and Lee, J. P. (2001) Exposing Asymmetry between Monomers in Alzheimer's Amyloid Fibrils via Reductive Alkylation of Lysine Residues, *J. Am. Chem. Soc. 123*, 6728−6729.
69. Kheterpal, I., Zhou, S., Cook, K. D., and Wetzel, R. (2000) Aβ amyloid fibrils possess a core structure highly resistant to hydrogen exchange, *Proc. Natl. Acad. Sci. U.S.A. 97*, 13597−13601.
70. Kheterpal, I., Williams, A., Murphy, C., Bledsoe, B., and Wetzel, R. (2001) Structural Features of the Aβ Amyloid Fibril Elucidated by Limited Proteolysis, *Biochemistry 40*, 11757−11767.
71. Kheterpal, I., Lashuel, H. A., Hartley, D. M., Walz, T., Lansbury, P. T., Jr., and Wetzel, R. (2003) Aβ protofibrils possess a stable core structure resistant to hydrogen exchange, *Biochemistry 42*, 14092−14098.
72. Roher, A. E., Baudry, J., Chaney, M. O., Kuo, Y. M., Stine, W. B., and Emmerling, M. R. (2000) Oligomerization and Fibril Assembly of the Amyloid-β Protein, *Biochim. Biophys. Acta 1502*, 31−43.
73. Wang, S. S.-S., Tobler, S. A., Good, T. A., and Fernandez, E. J. (2003) Hydrogen Exchange-Mass Spectrometry Analysis of β-Amyloid Peptide Structure, *Biochemistry 42*, 9507−9514.
74. Pike, C. J., Overman, M. J., and Cotman, C. W. (1995) Amino-terminal deletions enhance aggregation of beta-amyloid peptides in vitro, *J. Biol. Chem. 270*, 23895−23898.
75. Hilbich, C., Kisters-Woike, B., Reed, J., Masters, C. L., and Beyreuther, K. (1991) Aggregation and secondary structure of synthetic amyloid β A4 peptides of Alzheimer's disease, *J. Mol. Biol. 218*, 149−163.
76. Hesse, L., Beher, D., Masters, C. L., and Multhaup, G. (1994) The βA4 amyloid precursor protein binding to copper, *FEBS Lett. 349*, 109−116.

BI047611E